Seismic vulnerability of Multi-span bridges: An analytical perspective

S. Mangalathu, J. Jeon, F. Soleimani & R. DesRoches

Department of Civil Engineering, Georgia Institute of Technology, Atlanta, USA.

J. Padgett

Department of Civil Engineering, Rice University, Houston, Texas, USA.

J. Jiang

Department of Civil Engineering, Zhejiang University City College, Hangzhou, China.

ABSTRACT: Although the seismic vulnerability of bridges is significantly reduced with the advancement of design philosophies, the susceptibility of damage to the existing bridge stock is of great concern to the earthquake research community. Fragility curves are powerful tools used in the seismic risk assessment of bridges. This study presents the fragility curves for multi-span bridges accounting for the uncertainties in the structural and material attributes. Nonlinear time history analysis is conducted using three dimensional finite element bridge models developed in the OpenSees platform containing realistic representations of bridge components including columns, super structure, bearings, abutments, and pounding (impact) behavior. The probabilistic seismic demand model computed from the time history analysis is convolved with component limit states to generate fragility curves. The current study also compares the fragility curves generated by the classical approach with the surrogate modeling or parameterized approach. The coefficients suggested by the parameterized approach in this study can be used to generate bridge specific fragility curves. The study also investigates the influence of seismic detailing on multi-span bridges.

1 INTRODUCTION

Bridges are considered as the lifeline of modern transportation networks. Damage to bridges after an earthquake pose a serious threat to the immediate recovery efforts and can incur large economic losses. An effective and increasingly popular technique to determine the effects of earthquake ground motions on the bridge system as well as various bridge components is fragility analysis. A fragility curve is a conditional probability that gives the likelihood that a structure or component will meet or exceed a certain level of damage for a given ground motion intensity. Various researchers (Choi et al. 2004; Mackie & Stojadinović 2005; Padgett 2007; Ramanathan et al. 2015; Jeon et al. 2015) have developed the fragility curves for bridge structures (called hereafter as classical approach). However, very few studies have been carried out for the fragility curves of multi-span box girder bridge classes. The current study bridges this gap by generating fragility curves for multi-span box girder bridge classes. Contrary to the previous studies, the fragility curves are developed in this study using surrogate modeling techniques (called hereafter as parameterized fragility curves), (Dukes 2013; Ghosh et al. 2013; Rokneddin et al. 2014). The parameterized fragility curves use multi-dimensional surrogate models in conjunction with logistic regression techniques to develop the component as well as system fragility curves. Thus it helps to create bridge specific fragility curves, and can potentially benefit from the new data available from the field investigations. The logistic regression coefficients estimated in the current study can be used to generate bridge specific fragility curves for various classes of multi-span bridges. The study also investigates the effect of seismic detailing on the seismic vulnerability of the multi-span bridges by the comparison of fragility curves for bridges with and without ductile detailing.

One of the notable differences between the seismically and non-seismically designed bridges with the evolution of seismic design practice is the detailing aspects of columns (Ramanathan 2012a). Non-seismically designed bridges (constructed prior to 1970) are designed primarily to carry gravity loads and are often inadequately detailed to resist seismic forces. They are highly vulnerable due to the

inadequate shear strength, insufficient splicing at the intersection of columns and footing and/or inadequate confinement in the flexural hinge zones. In comparison to the non-seismically designed bridges, seismically designed bridges (constructed post 1970) have greater splice lengths and transverse reinforcement ratios in the longitudinal and lateral direction. The effects of inadequate shear strength and lap splice mode of failure of the bridge columns are not investigated in this study. The comparison of the analytical results with the past events is beyond the scope of this research and is a part of the ongoing research.

2 MODELING OF BRIDGE COMPONENTS

The typical layout of a multi-span box girder bridge is shown in Figure 1. The structural analysis phase of the methodology is performed using the Finite element package called OpenSees (Mazzoni, et al. 2006). The superstructure is modeled using elastic beam-column elements with mass lumped along the centerline and the monolithic solid diaphragms are modeled using transverse rigid elements. The properties of deck elements are calculated based on composite section properties to account for the presence of box girders. Rigid links are used to connect the top of the column to the solid diaphragm. Displacement beam-column elements with fiber cross-sections are used for modeling columns. A distributed plasticity element is used to capture the nonlinear hysteretic behavior of the column. The contact element developed by Muthukumar & DesRoches (2006), which explicitly accounts for the loss of hysteretic energy, is used to model the pounding between the decks. The longitudinal response of the abutments includes passive and active resistance. The passive resistance is provided by the backfill soil and the piles, while the active resistance and the transverse resistance are provided only by the piles. The passive response of the abutment backwall is simulated using the hyperbolic soil model proposed by (Shamsabadi & Yan 2008). Trilinear springs stemming from the recommendations of (Choi 2002) are used to model the piles. Readers are advised to refer to Ramanathan (2012b) for a more detailed and in-depth explanation of the modeling of various bridge components.

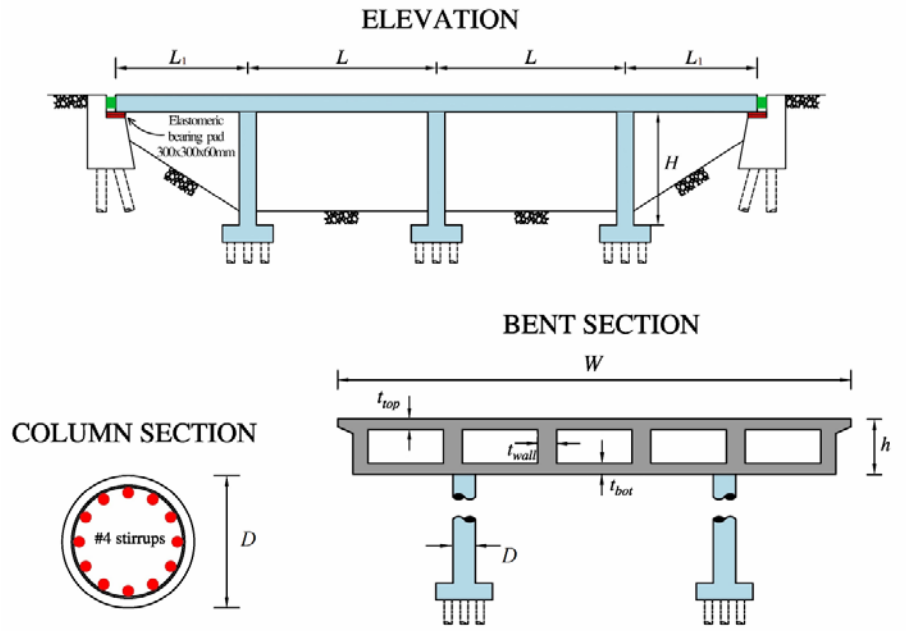

Figure 1. Typical layout of a multi-span bridge

The ratio of approach span to main-span is fixed as 0.70 and the column diameter (D) is fixed as 60 in. (1.5 m). Column footings are assumed to be fixed at the base. The effect of foundation flexibility and soil-structure interaction on the fragility curves is not considered and is a part of the ongoing study. The reduced spacing of the stirrups in the transverse direction is considered as the difference between seismically and non-seismically designed bridges. Number #4 hoops (0.25 in. dia. bar) at a spacing of 12 in. on center is assumed as the transverse reinforcement for non-seismically designed bridges while for seismically designed bridges, it is assumed as #4 hoops @ 3 in., on center. Bearings are assumed to

be of size 14 × 14 × 2.5 in. (300 × 300 ×60 mm). The geometric and material properties are computed based on the plan review of multi-span box girder bridges.

It's important to have a wide range of ground motions with a large variation of peak ground accelerations to ensure the evaluation of a sufficient range of bridge responses. A suite of 160 ground motions is adopted in this study. The ground motions are selected from the PEER database of far field earthquakes with magnitude greater than 6.5 and peak ground acceleration greater than 0.2 g such that it yields a desired variation of bridge responses. Figure 2 shows the histogram of the PGA values and the response spectrum of the selected ground motions. The ground motions are applied along the longitudinal axis of the bridge. Statistically significant, yet nominally identical 160 - 3D bridges are developed based on the Latin Hypercube Sampling across the range of input parameters (Table 1, Ramanathan 2012b; Mangalathu et al. 2015) consistent with the number of ground motions. The generated bridge models are paired randomly with the selected 160 ground motions to create a bridge model-ground motion pair. Non-linear time history analysis (NLTHA) is carried out on each bridge model and the peak component responses are noted to determine the relationship between the peak demands and the input parameters

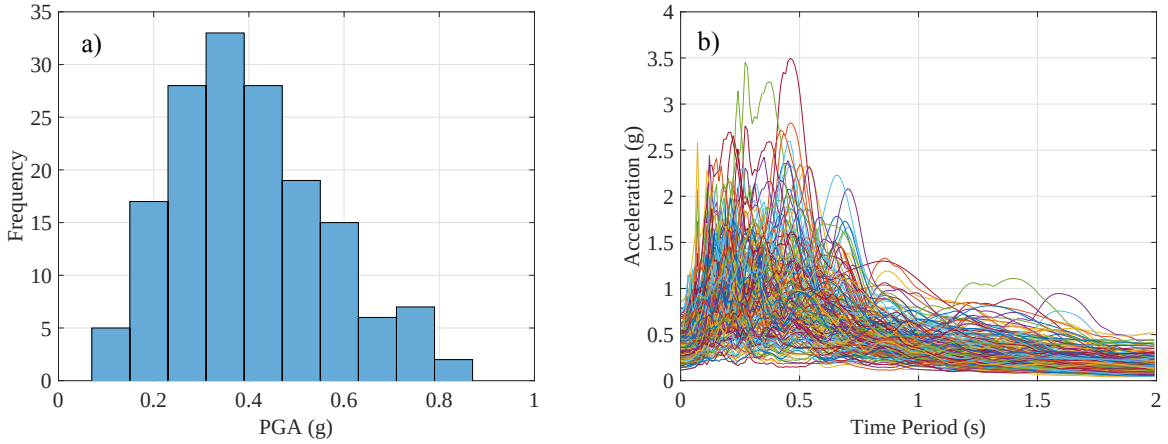

Figure 2. a) Histogram of the PGA values of the ground motion suite, b) Acceleration response spectrum of the ground motion suite

Table 1: Distribution of base-model parameters for era 11 single-frame concrete box-girder bridges.

Parameter	Units	Distribution Type	Distribution parameters*	
			α	β
Span length (p_1)	feet	Normal	82.0	8.2
Deck width (p_2)	feet	Uniform	32.5	98.5
Column height (p_3)	feet	Normal	16.5	0.16
Number of columns per bent (p_4)	-	Uniform**	1	4
Longitudinal reinforcement ratio (p_5)	%	Uniform	1	3.5
Concrete strength (p_6)	ksi	Normal	5	0.63
Steel strength (p_7)	ksi	Lognormal	4.21	0.08
Shear modulus of bearing pad (p_8)	ksi	Uniform	0.08	0.25
Number of spans (p_9)	-	Uniform**	4	6

*α and β are the parameters of the distribution. These denote mean and standard deviation for a normal distribution, lower and upper bound in case of uniform distribution and mean and standard deviation of the associated normal distribution (in log space) in the case of a lognormal distribution.
**only integer values

3 DEMAND AND CAPACITY MODELS

Fragility curves consider the probability that the seismic demand (D) placed on the structure exceeds

the capacity (C) conditioned on a chosen intensity measure (IM) representative of the seismic loading. The demand aspect of the fragility function is represented by the probabilistic seismic demand computed using the results of non-linear time history analysis and regression analysis. The capacity models are described by a two-parameter lognormal distribution with median, S_c and dispersion, β_c (β_c is assigned as 0.35 in a subjective manner due to lack of sufficient information and adopted as same across the components and the respective damage states). The general description of system level damage states of the bridge and the capacity limit states of the bridge components are given in Table 2 and Table 3 respectively (Ramanathan 2012b). The capacity limit states are shown in Table 3 for all the individual bridge components that are susceptible to damage during ground shaking.

Table 2. General description of system level damage states for bridges (Ramanathan 2012b).

Bridge system damage states	**Slight**	**Moderate**	**Extensive**	**Collapse**
Likely Immediate Post-Event Traffic State	Open to normal public traffic – No Restrictions	Open to Limited public traffic – speed/weight/lane restrictions	Emergency vehicles only – speed/weight/lane restrictions	Closed (until shored/braced) – potential for collapse
Traffic Operation Implications				
Is closure/detour needed?	Very unlikely	Unlikely	Likely	Very likely
Are traffic restrictions needed?	Unlikely	Likely	Very Likely	Very Likely - Detour
Emergency Repair Implications				
Is shoring/bracing needed?	Very unlikely	Unlikely	Likely	Very likely
Is roadway levelling needed?	Unlikely	Likely	Very Likely	Very Likely - Detour

Table 3. Capacity limit state values of various bridge components (Ramanathan, 2012b).

Component	**Median values, S_c**				β_c
	Slight	**Moderate**	**Extensive**	**Collapse**	
Column curvature ductility (k_1)	0.8(1.0)*	0.9(4.0)	1.0(8.0)	1.2(12.0)	0.35
Abutment seat displacement : 12 – 18 inch seat(in., k_2)	1.0(2.0)	3.0(6.0)	6.0(10.0)	9.0(15.0)	0.35
Maximum deck displacement (in., k_3)	4.0(4.0)	12.0(12.0)	-	-	0.35
Active abutment response (in., k_4)	1.5(1.5)	4.0(4.0)	-	-	0.35
Joint seal displacement (in., k_5)	0.75(4.0)	10.0(10.0)	-	-	0.35

* Values in parenthesis corresponds to limit states of modern era bridges

4 PARAMETERIZED FRAGILITY CURVES

Fragility curves generated in this study are based on the parameterized fragility approach developed by the researchers (Dukes 2013, Ghosh et al. 2013; Rokneddin et al. 2014). In comparison to the classical fragility analysis (Choi et al. 2004; Ramanathan et al. 2015) which considers ground motion intensity as the only input parameter, the demand models in the parameterized fragility curves are conditioned on all the input parameters. Hence, the parameterized fragility approach can also be used to create bridge specific fragility curves. A brief outline of this method is given in this section and the readers are advised to refer to Ghosh et al. (2013) for a more detailed explanation. We adopted multiple-linear regression as the surrogate model in the current study due to its simplicity and easiness in implementation. The evaluation of various meta-models for the generation of demand models for multi-span bridges albeit important is out of the scope of this study and is a part of an ongoing research.

The main steps of the parameterized fragility curves connecting the input parameters ($p_1,\ldots,p_9, S_a$) to the output measures ($k_1,\ldots,k_7$) are outlined below:

Step 1: Perform multiple linear regression analysis for each component (k_i, i = 1,…,5) with the input parameters ($p_1,\ldots,p_9$, S_a) and compute the regression coefficients.

Step 2: Generate N number of demand estimates (1 million in this study) for each component, k_i, using their respective regression model by generating N values of randomly generated input parameters based on their probabilistic distribution.

Step 3: Generate N capacity values for a specific damage state for each bridge component based on their corresponding capacity limit states (Table 3).

Step 4: Obtain the binary survive-failure vector by comparing the capacity values (step 3) with the demand values (step 2).

Step 5: Conduct a logistic regression on the survive-failure vector to determine the k^{th} component probability model, conditioned on the input parameters as

$$PF_{k|S_a,p_1,p_2,..p_9} = \frac{e^{\theta_{k,0}+\theta_{k,S_a}\ln(S_a)+\sum_{j=1}^{9}\theta_{kj}\ln(p_j)}}{1+e^{\theta_{k,0}+\theta_{k,S_a}\ln(S_a)+\sum_{j=1}^{9}\theta_{kj}\ln(p_j)}} \quad (1)$$

where, $\theta_{k,0,}$ $\theta_{k,sa,}$ and $\theta_{k,j's}$ (j = 1,…,9) are the logistic regression coefficient's of the k^{th} bridge component.

Step 6: Assuming a series system assumption, estimate the system level binary-survive failure vectors. The system level failure probability can be obtained by the logistic regression analysis for the system level binary-survive failure vectors.

$$PF_{SYS|S_a,p_1,p_2,..p_9} = \frac{e^{\theta_{SYS,0}+\theta_{SYS,S_a}\ln(Sa)+\sum_{j=1}^{9}\theta_{SYS,j}\ln(p_j)}}{1+e^{\theta_{SYS,0}+\theta_{SYS,S_a}\ln(Sa)+\sum_{j=1}^{9}\theta_{SYS,j}\ln(p_j)}} \quad (2)$$

where, $\theta_{SYS,0,}$ $\theta_{SYS,sa,}$ and $\theta_{SYS,j's}$ (j = 1,…,9) are the logistic regression coefficient's for the system failure.

Step 7: For a particular bridge with input parameters, $p_1,\ldots, p_9$, the classical one-dimensional fragility curves can be obtained as

$$PF_{SYS|S_a} = \int_{p_1}\int_{p_2}\ldots\int_{p_9} \frac{e^{\theta_{SYS,0}+\theta_{SYS,S_a}\ln(S_a)+\sum_{j=1}^{9}\theta_{SYS,j}\ln(p_j)}}{1+e^{\theta_{SYS,0}+\theta_{SYS,S_a}\ln(S_a)+\sum_{j=1}^{9}\theta_{SYS,j}\ln(p_j)}} f(p_1)\ldots f(p_9)\,dp_1\ldots dp_9 \quad (3)$$

where $f(p_1),\ldots, f(p_9)$ are the probability density parameters for parameters, $p_1,\ldots, p_9$.

5 RESULTS AND DISCUSSION

The fragility curves generated by the classical method and the parameterized way for various damage states were compared and are shown in Figure 3. It is observed that the fragility curves generated by parameterized approach are similar to those obtained using classical approach. However, a significant difference is noted for the extensive and complete damage state for the modern era fragility curves. The advantage of the parameterized fragility curves lies in the fact that for a specific bridge with deterministic input parameters ($p_1,\ldots, p_9$), the fragility curves can be computed easily using Equation 3 with the coefficients given in Table 4. Table 4 gives the logistic regression coefficient for the system level damage for various damage states.

Table 4. Logistic regression coefficients for the system damage for various damage states

	Damage states	$\theta_{k,0}$	θ_{k,S_a}	θ_{k,p_1}	θ_{k,p_2}	θ_{k,p_3}	θ_{k,p_4}	θ_{k,p_5}	θ_{k,p_6}	θ_{k,p_7}	θ_{k,p_8}	θ_{k,p_9}
Old era	Slight	-7.05	7.62	0.77	8.44	1.03	-0.58	-4.11	0.25	-5.63	-0.80	-1.89
	Moderate	-26.2	6.38	1.28	5.15	1.33	-0.52	-4.75	-3.74	0.62	-0.04	-1.73
	Extensive	-26.9	6.33	1.48	5.56	1.28	-0.49	-4.67	-3.38	0.08	-0.12	-1.66
	Collapse	-27.8	6.39	1.50	5.02	1.32	-0.54	-4.77	-3.86	0.60	-0.01	-1.80
Modern era	Slight	-12.5	6.65	1.74	4.91	1.85	-0.98	-5.21	0.05	-5.46	-0.13	-1.31
	Moderate	-18.1	6.49	1.42	4.63	1.84	-0.99	-5.01	-0.23	-5.08	-0.04	-1.22
	Extensive	-21.1	6.88	1.60	5.50	1.79	-1.07	-4.91	-0.01	-5.87	-0.26	-1.38
	Collapse	-23.8	6.61	0.88	6.07	2.72	-0.93	-5.43	-0.88	-6.39	-0.64	-1.10

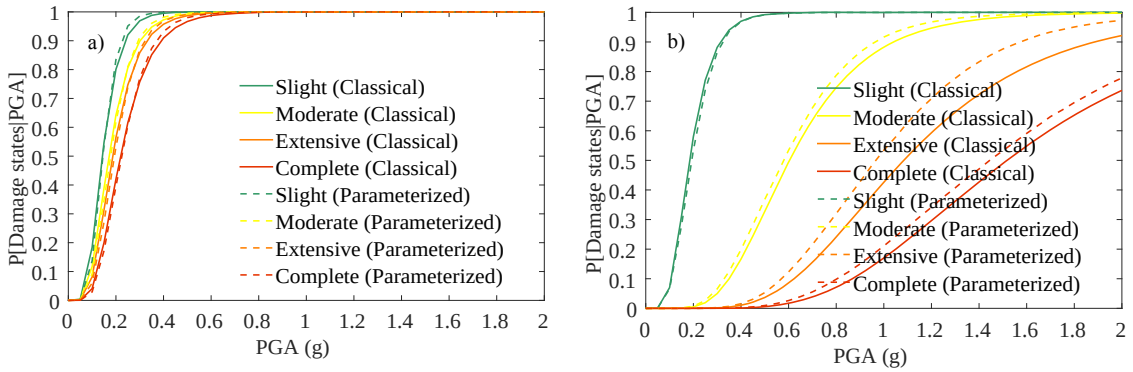

Figure 3. Comparison of the classical and parametrized fragility curved for various damage states: a) Old era, b) Modern era

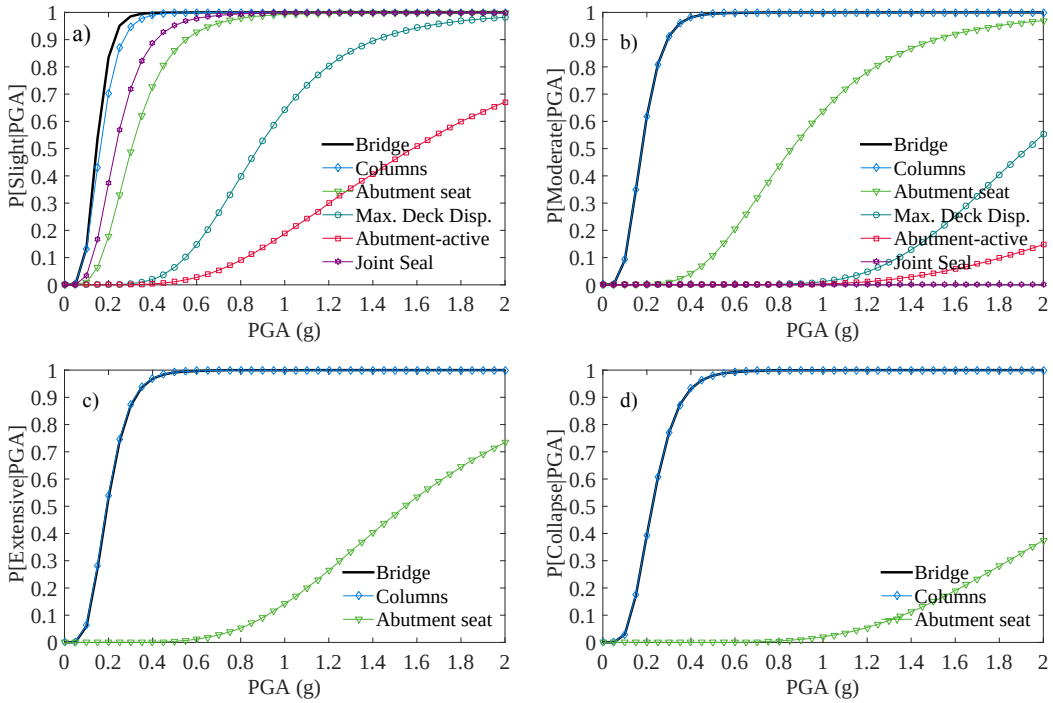

Figure 4. Bridge and component system fragility curves for multi-span box girder bridges for old era's a) Slight, b) Moderate, c) Extensive and d) Collapse.

One simple technique to evaluate the difference in the fragility curve is to evaluate the relative change in the median value of the fragility curves. An increase in the median value means a less vulnerable structure while a decrease in the median value indicates a more vulnerable structure. The median value of the fragility curves for modern era bridges are much larger than the old era bridges for all the limit

states. From the results presented in Figure 3, it is observed that seismic vulnerability is significantly reduced with the implementation of seismic design principles in the design. The median value of fragility curves for distinct damage states of old era bridges (Figure 3a) are so close due to its limited capacity resulting from the non-ductile design (Table 3). The effect of ductile design on the various damage states is clearly visible with the dispersion of fragility curves for modern era bridges (Figure 3b).

The system and component fragility curves for the multi-span bridges for various damage states for the old era and modern era are shown in Figure 4 and Figure 5 respectively. From the results presented in Figure 4 and Figure 5, it is noted that the columns and abutment seat are the most vulnerable components. The component fragilities (columns, abutments, bearings etc.) are integrated into the system fragility using the approach mentioned in Section 4. The components such as abutment active, deck displacement, and joint seal have less contribution to the overall system vulnerability. The vulnerability of the system as well as the components decreases with the evolution of seismic design principles.

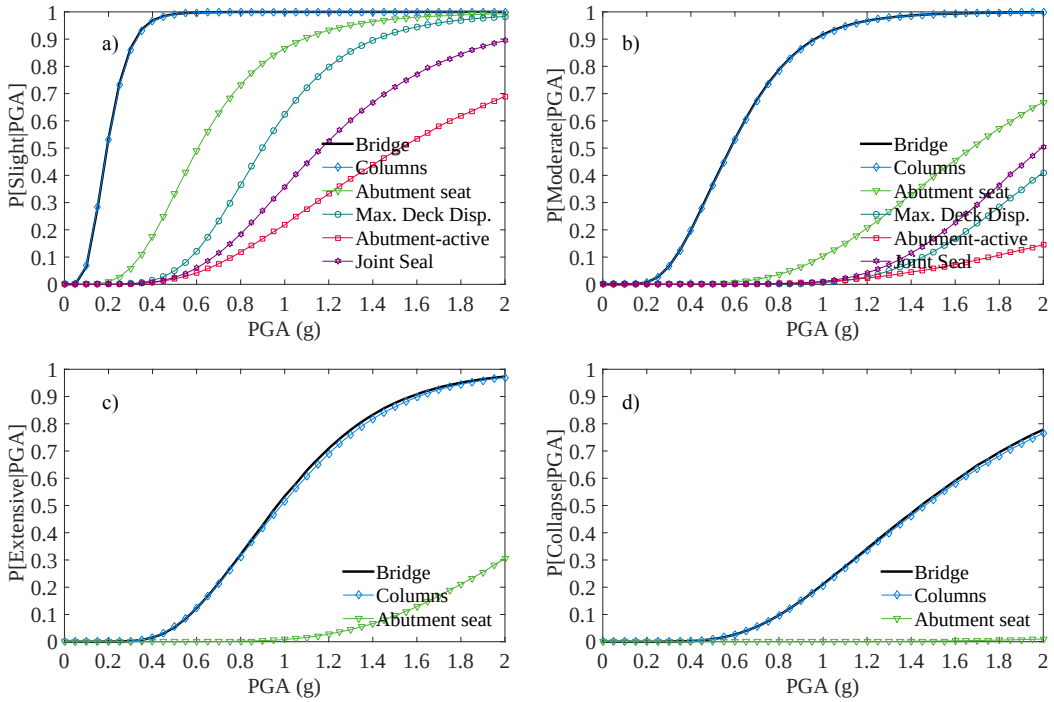

Figure 5. Bridge and component system fragility curves for multi-span box girder bridges for modern era's a) Slight, b) Moderate, c) Extensive and d) Collapse.

6 CONCLUSION

In this study, two methods of fragility analysis i.e., classical and parameterized fragility approach are compared. In addition, the effects of earthquake ground motions on the bridge system as well as bridge components are also evaluated using fragility analysis. Three dimensional finite element models of the bridge incorporating both material as well as geometric nonlinearities are developed in the OpenSees platform that contain realistic representations of bearings, abutments, and pounding of adjacent deck segments using nonlinear springs. Probabilistic seismic demand models generated using NLTHA are convolved with limit states to develop the component and system fragility curves.

It is observed that the integrated parameterized fragility curves and classical fragility curves are in good agreement for the multi-span bridges considered in the current study and the coefficients of the parameterized fragility curves generated can be used to generate bridge specific fragility curves. The transition of seismic vulnerability with the evolution of seismic design practices is gauged in the current study through the comparison of fragility curves for old and modern eras. The study shows that

seismic vulnerability of the bridges is reduced significantly with the evolvement of seismic design philosophy.

Acknowledgement

The authors would like to thank the anonymous reviewers for their valuable comments and suggestions to improve the quality of the paper.

REFERENCES

Choi E. 2002. Seismic analysis and retrofit of mid-America bridges. *Ph.D Thesis*, Georgia Institute of Technology, Atlanta, Georgia.

Choi E., DesRoches R. & Nielson B. 2004. Seismic fragility of typical bridges in moderate seismic zones. *Engineering Structures*. Vol. 26(2). 187-199.

Ghosh J., Padgett J.E. & Dueñas-Osorio L. 2013. Surrogate modeling and failure surface visualization for efficient seismic vulnerability assessment of highway bridges. *Probabilistic Engineering Mechanics*. Vol. 34. 189-199.

Dukes, J. D. 2013. Application of bridge specific fragility analysis in the seismic design process of bridges in california. *Ph.D Thesis*, Georgia Institute of Technology, Atlanta, Georgia.

Jeon, J.-S., Shafieezadeh, A., Lee, D. H., Choi, E., & DesRoches, R. (2015). Damage assessment of older highway bridges subjected to three-dimensional ground motions: Characterization of shear-axial force interaction on seismic fragilities. *Engineering Structures*, Vol. 87, 45-57.

Mackie K.R. & Stojadinović B. 2005. Fragility basis for California highway overpass bridge seismic decision making: *Pacific Earthquake Engineering Research Center*, College of Engineering, University of California, Berkeley.

Mangalathu S., Jeon J., DesRoches R. & Padgett J.E. 2015. Analysis of Covariance to Capture the importance of bridge attributes on the probabilistic seismic demand model. *Proc. 15th Pacific Conference on Earthquake Engineering, Sydney. 6-8 Novemeber 2015*. Australia.

Mazzoni S., McKenna F., Scott M.H. & Fenves, G.L. 2006. OpenSees command language manual. *Pacific Earthquake Engineering Research (PEER) Center*.

Muthukumar S. & DesRoches R. 2006. A Hertz contact model with non-linear damping for pounding simulation. *Earthquake Engineering & Structural Dynamics*. Vol. 35(7). 811-828.

Padgett J.E. 2007. *Seismic vulnerability assessment of retrofitted bridges using probabilistic methods*. *Ph.D Thesis*, Georgia Institute of Technology, Atlanta, Georgia.

Ramanathan, K., DesRoches, R., & Padgett, J. E. 2012a. A comparison of pre- and post-seismic design considerations in moderate seismic zones through the fragility assessment of multispan bridge classes. *Engineering Structures*, Vol. 45, 559-573

Ramanathan K.N. 2012b. *Next generation seismic fragility curves for California bridges incorporating the evolution in seismic design philosophy*. *Ph.D Thesis*, Georgia Institute of Technology, Atlanta, Georgia.

Ramanathan K., Padgett J.E. & DesRoches R. 2015. Temporal evolution of seismic fragility curves for concrete box-girder bridges in California. *Engineering Structures*. Vol. 97. 29-46.

Rokneddin K., Ghosh J., Dueñas-Osorio L. & Padgett J.E. 2014. Seismic Reliability Assessment of Aging Highway Bridge Networks with Field Instrumentation Data and Correlated Failures, II: Application. *Earthquake Spectra*. Vol. 30(2). 819-843.

Shamsabadi, A., & Yan, L. 2008. Closed-form force-displacement backbone curves for bridge abutment-backfill systems. *Proc. of the Geotechnical Earthquake Engineering and Soil Dynamics IV Congress, American Society of Civil Engineers*. *18-22 May*, Sacramento, California